Eur. J. Mineral.
2007, **19**, 419–427

Schafarzikite from the type locality Pernek (Malé Karpaty Mountains, Slovak Republic) revisited

Jiří SEJKORA[1,*], Daniel OZDÍN[2], Jiří VITÁLOŠ[3], Peter TUČEK[4], Jiří ČEJKA[1] and Rudolf ĎUĎA[5]

[1] Department of Mineralogy and Petrology, National Museum, Václavské nám. 68, 115 79, Praha 1, Czech Republic
*Corresponding author, e-mail: jiri_sejkora@nm.cz
[2] Department of Mineralogy and Petrology, Faculty of Natural Sciences, Comenius University, Mlynská dolina, 84215 Bratislava, Slovak Republic
[3] Šenkvická cesta 9, 90201 Pezinok, Slovak Republic
[4] Klíž 80, 95845 Vel'ký Klíž, Slovak Republic
[5] Eastern Slovak Museum, Hviezdoslavova 3, 04136 Košice, Slovak Republic

Abstract: A rare mineral schafarzikite, an oxide of Fe^{2+} and Sb^{3+}, was found after more than 80 years at the type locality near Pernek (Malé Karpaty Mountains, Slovak Republic). Crystals, druses, and crusts of schafarzikite occur on fractures in quartz-carbonate-stibnite hydrothermal ores. The Sb mineralization is bound to black shales and phyllites in a zone of actinolitic rocks. Associated minerals include ankerite, berthierite, stibnite, valentinite, kermesite, senarmontite, and gypsum. Prismatic crystals of schafarzikite are 0.1–1.0 mm, rarely up to 1.5 mm large, with the dominant forms {110}, {121}, {112}, {010}, {221}, {131}, and {231}. The optical properties are: uniaxial, with relatively strong pleochroism in red-brown tints; refraction indices higher than 1.74; the average refraction index, calculated from the Gladstone-Dale equation, is 2.001. The physical properties of schafarzikite from Pernek are: dark brown to black color, adamantine to metallic luster, brown streak; translucent (brown to orange) in very thin fragments; good {100} cleavage and perfect cleavage along unindexed planes parallel to z axis, tenacity-brittle; VHN_{10g} microhardness = 251 and 278 kp/mm^2 (for two cuts with differing orientation), corresponding to Mohs' hardness of 3.5–4; calculated density D_x = 5.507 g/cm^3. The electron microprobe analysis gave FeO 19.38, ZnO 0.02, PbO 0.02, Sb_2O_3 80.36, As_2O_3 0.55, Bi_2O_3 0.16, SO_2 0.04, and calculated formula $Fe_{0.97}(Sb_{1.99}As_{0.02})_{\Sigma 2.01}O_4$. The XRD pattern was indexed in a tetragonal setting, with refined unit-cell parameters are a = 8.6073(2), c = 5.9093(3) Å, V = 437.80(2) Å^3, $c : a$ = 0.6865. Thermogravimetric (TG) curve shows mass gain of 1.62 wt. % in the range 20–580 °C, and 5.28 wt. % in the range 580–850 °C caused by Fe^{2+} and Sb^{3+} oxidation, respectively. The product of TG analysis is a phase isostructural with rutile. A tentative assignment of FTIR and Raman spectra of schafarzikite is given. Schafarzikite from Pernek most likely crystallized from late oxidizing hydrothermal fluids. Hence, it is not a weathering product, as assumed previously.

Key-words: schafarzikite, X-ray diffraction, thermogravimetry behavior, infrared spectroscopy, Raman spectroscopy, Sb-deposit Pernek.

Introduction

Schafarzikite, ideally $Fe^{2+}Sb_2^{3+}O_4$, is a rare mineral of Sb hydrothermal mineral deposits which formed from relatively oxidizing fluids. The mineral was first described by Krenner (1921) from the Sb deposit Pernek in Malé Karpaty Mts., Slovak Republic. It was named after Ferenc Schafarzik (1854–1927), a Hungarian mineralogist (Blackburn & Dennen, 1997).

Krenner (1921; 1923) proposed schafarzikite as a new mineral only by studying its crystal morphology and having an incorrect chemical analysis that gave composition nFeO·P_2O_3. He noted that schafarzikite is accompanied by stibnite, kermesite, senarmontite, valentinite, and younger calcite and aragonite. Tokody (1925) reports for schafarzikite more precise crystallographic data, optical properties, hardness, and specific gravity. Hueber (1932) published the first chemical analysis of this mineral and proposed an ideal composition of $Fe_5Sb_4O_{11}$. Zemann (1951) solved the crystal structure of schafarzikite in the space group $P4_2/mbc$ and used these data for determination of its ideal composition as $FeSb_2O_4$. The crystal structure was refined by Fischer & Pertlik (1975) in the same space group to R = 0.036. Fischer & Pertlik (1975) also reported incomplete semi-quantitative results of chemical analyses. There are no other published accounts of schafarzikite from Pernek and no reports of finding this mineral in Pernek since the 1920's.

Schafarzikite was also described from Buca della Vena in the Apuan Alps in Italy (Mellini *et al.*, 1979), from Lac

0935-1221/07/0019-1723 $ 4.05

DOI: 10.1127/0935-1221/2007/0019-1723

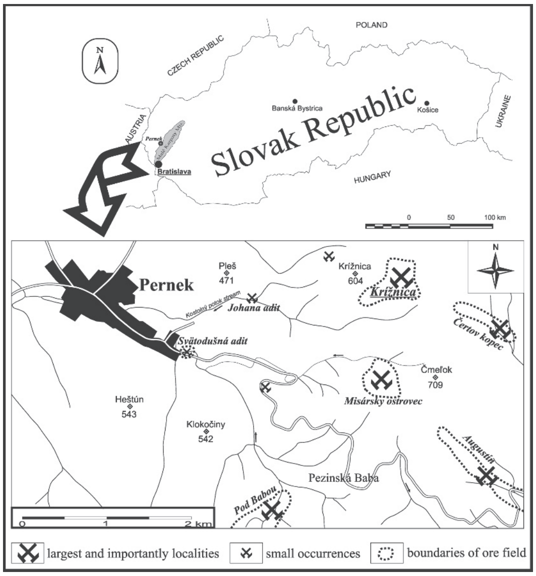

Fig. 1. A map showing the location of abandoned mines in the vicinity of the village of Pernek (Malé Karpaty Mountains, Slovak Republic).

Nicolet mine, Canada (Robinson & Normand, 1996), from Stabiello Alps, Italy (Callegari & Mattioli, 2000), and from the Kharma Sb deposit in Bolivia (Dill *et al.*, 1995).

In 2002, we found numerous specimens of schafarzikite at the type locality Pernek-Krížnica. These samples are very similar to the original material collected by Krenner, and represent the first findings of this rare mineral after more than eighty years.

Geological setting

The Sb deposit Pernek - Krížnica is situated about 3 km east from the village of Pernek (Fig. 1), on the eastern slopes of the hill Krížnica (604 m) in the Malé Karpaty Mountains (Slovak Republic). Malé Karpaty mountains are built by the pre-Alpine basement, its Mesozoic cover, and superficial nappe complexes (Plašienka *et al.*, 1991). The pre-Alpine (Tatric) basement includes two formations. The lower formation is dominated by pelito-psammitic, flysch-like metamorphosed rocks of Silurian to Lower Devonian age. This formation gradually fades into the upper, volcano-sedimentary formation of Lower to Mid-Devonian age (Planderová & Pahr, 1983). The upper formation is built mostly by black shales, carbonates, basalts and tuffs, less frequently by gabbros and gabbrodiorites. The age of the earliest metamorphic event in the Pezinok-Pernek crystalline complex was estimated to 380 ± 20 Ma (Cambel *et al.*, 1990). Isotopic analyses of granitoid rocks from the Malé Karpaty Mts. gave an age of 348 ± 4 Ma (Cambel *et al.*, 1990).

Post-Hercynian evolution of the Malé Karpaty Mts. was characterized by extensive sedimentation and the Alpine orogeny (Plašienka *et al.*, 1991). The significant reduction of sedimentation space in Mid-Cretaceous was associated with thrusting and folding. The basin widened westward during Paleogene, and the Neogene faults finalized the horst structure of this mountain range, as we know it today.

Analytical procedures

Quantitative chemical analyses of all studied phase were acquired by an electron microprobe Cameca SX100 in wavelength dispersive mode (acceleration voltage 20 kV, current sample 20 nA, beam diameter 0.75–5 µm). The standards and wavelengths used were: Bi_2Se_3 (Bi Lα), PbS (Pb Mα), ZnS (Zn Kα), Sb_2S_3 (Sb Lβ), FeAsS (As Kβ), Sn (Sn Lβ), CdS (Cd Lα), $CuFeS_2$ (Cu Kα, Fe Kα, S Kα), hematite (FeKα), wollastonite (Ca Kα), NaCl (Cl Kα). Arsenic concentrations in some of the studied minerals are close to detection limit, and the measured values are dubious. The concentrations of Mg, Mn, Ti and Na were below the detection limits. Scanning electron microscope (SEM) images were taken with a Tesla BS 340 SEM with acceleration voltage of 20 kV and beam current of 10 nA. Obtained SEM images were compared with forms modeled with the Shape program (www.shapesoftware.com). This was applied for the determination of crystal forms of schafarzikite.

The X-ray powder diffraction (XRD) patterns were obtained from hand-picked samples using an HZG4-AREM/Seifert diffractometer, with a Cu source operated at a current of 40 mA and voltage of 50 kV. For unit-cell parameters determination (Burnham program, 1962), the XRD patterns were collected in an angular range of 12°–101° 2θ, with step size 0.02° 2θ and dwell 6 s. They were indexed by comparison with a powder pattern calculated (program Lazy Pulverix program, Yvon *et al.*, 1977) from published crystal structures.

Thermogravimetric analysis was carried out by a Stanton Redcroft TG 750 Thermobalance. The sample (2.968 mg) was heated from room temperature to 850 °C at a heating rate 10 °C min^{-1} in flowing air (10 ml·min^{-1}). VHN microhardness was determined with a PMT-3 microhardness measurement device with a Vickers diamond pyramid and halite crystals as a standard.

The FTIR spectrum in the range 1000–400 $cm^{-1}$was obtained with the FTIR Nicolet 740 type apparatus using the conventional KBr-disk technique. The Raman spectrum in the range 1000–100 cm^{-1} was collected with a dispersive Raman spectrometer Labram HR (Jobin Yvon) and confocal Olympus microscope. The Raman signal was excited by a 785 nm laser and detected with a multichannel air-cooled CCD camera. The laser power at the sample was limited to 4 mW.

The ore mineralization and associated minerals

The ore mineralization at the deposit Pernek-Krížnica is associated with carbonaceous shales and phyllites in a zone of actinolitic metamorphic rocks. There are two types of ores at the deposit, one dominated by stibnite, the other

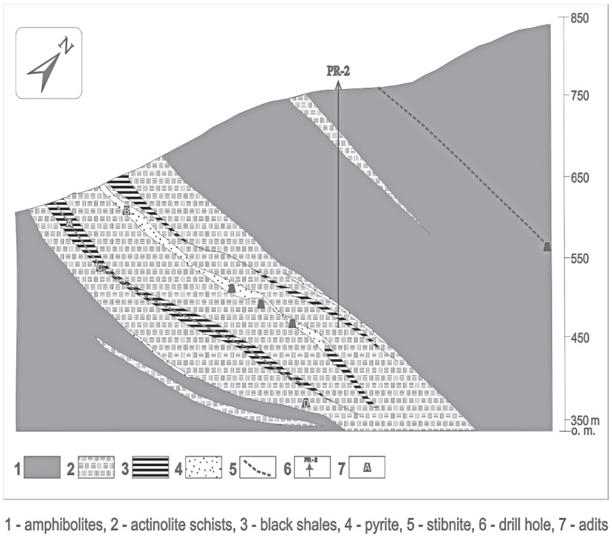

Fig. 2. Cross-section of the Sb deposit Pernek-Krížnica.

Table 1. Chemical composition of berthierite and stibnite from Pernek.

	Berthierite		Stibnite	
	mean	range	mean	range
Fe	11.83	11.37–12.23		
Cd	0.03	0.03–0.04		
Pb	0.08	0.02–0.15		
Sn	0.10	0.00–0.15	0.20	0.18–0.21
Sb	57.17	56.68–57.92	71.24	70.89–71.45
S	28.41	26.55–29.82	28.09	27.98–28.19
Cl	0.01	0.00–0.01		
Total	97.63		99.53	

one by pyrite. The mineralized stockworks (Cambel, 1959) contain abundant quartz and carbonates and their thickness varies between 0.5–1.0 m, rarely up to 4.0 m (Fig. 2). The stibnite-bearing stockworks have NW-SE strike, 40–60° dip to NE and are heavily sheared and brecciated. Hydrothermal alteration is responsible for abundant quartz, carbonates, pyrite, and chlorite in the rocks that host the mineralized stockworks (Cambel, 1959; Čillík *et al.*, 1959).

Cambel (1959) distinguished three precipitation stages at the Pernek deposit: (1) quartz-pyrite-arsenopyrite stage, (2) stibnite-carbonate-quartz stage, and (3) stibnite-kermesite stage. Review of known primary and supergene minerals of the Pernek deposit was given by Koděra *et al.* (1990).

The newly found specimens with schafarzikite represent rocks mineralized with stibnite and pyrite, locally silicified, or with quartz veinlets up to 1 cm thick. These mineral species were identified:

Ankerite is one of the earliest hydrothermal minerals. It forms small (< 1 mm) rhombohedral crystals with curved faces, almost unweathered, with light gray to yellowish color. The XRD patterns correspond to an intermediate member of the ankerite-dolomite series, *i.e.*, Mg-rich ankerite.

Berthierite was found only in few samples as massive to fine-grained dark gray aggregates, up to 1 cm large, impregnating the ores in the immediate vicinity of the schafarzikite aggregates. Rare acicular crystals of bertherite are up to 3 mm long and intergrown within translucent crystals of senarmontite (I). Refined unit-cell parameters ($a = 11.411(1), b = 3.7636(6), c = 14.158(1)$ Å) agree well with published data. Beside the principal elements Fe, Sb, and S, the acicular berthierite contains up to 0.15 wt. % of Cd, Pb, Sn, and Cl (Table 1). The formula calculated from our analyses is $Fe_{0.95}Sb_{2.10}S_{3.95}$, suggesting elevated Sb concentration in comparison with the ideal composition $FeSb_2S_4$. The high Sb concentration may be caused either by contamination of the analyzed material by the surrounding senarmontite, or by crystallization of berthierite from solutions unusually rich in Sb.

Table 2. Chemical composition of valentinite and senarmontite from Pernek.

	Valentinite		Senarmontite	
	mean	range	mean	range
CaO			0.01	0.00–0.01
FeO	0.01	0.00–0.04	0.07	0.00–0.15
As_2O_3	0.39	0.00–0.88		
Sb_2O_3	100.40	99.44–101.25	99.18	98.98–99.49
Bi_2O_3			0.03	0.00–0.05
SO_2	0.01	0.00–0.02		
Cl	0.01	0.00–0.02		
total	100.80		99.29	

Stibnite is one of the most abundant phases, with variable morphology. The most common are light grey aggregates, up to 1 cm large, which impregnate the rocks around fractures. Stibnite occurs frequently as one of the oldest minerals on the fractures; it is forming radiating crystal groups of steel gray acicular crystals with intense metallic luster. The acicular stibnite crystals are sometimes in parallel intergrowths with aggregates of valentinite (I). Small druses of 1–2 mm needle-like stibnite crystals in the fractures are rare. The identity of the mineral was confirmed by XRD analysis and unit-cell parameter refinement which gave $a = 11.314(6), b = 3.845(4), c = 11.218(7)$ Å. Stibnite is homogeneous and devoid of inclusions of other minerals, when viewed in back-scattered electron images. The chemical analyses showed the presence of the major elements Sb and S and a steady concentration of minor Sn (Table 1). The calculated formula $(Sb_{2.00}Sn_{0.01})_{\Sigma 2.01}S_{2.99}$ is very close to the ideal composition Sb_2S_3.

Valentinite is an abundant mineral, formed during at least two separate stages. The earlier valentinite (I) occurs as radiating groups of transparent white crystals, up to 1 cm long. These crystals form parallel overgrowths over the earlier acicular stibnite. Minute (< 2 mm) colorless transparent tabular crystals belong to the later valentinite (II). These crystals overgrow kermesite and schafarzikite. Valentinite shows perfect {110} cleavage that causes significant preferred orientation problems for the XRD analysis. Valentinite (I) has pearly, valentinite (II) adamantine luster. Beside Sb, the chemical analyses (Table 2) indicate only higher concentration of As up to 0.025 *apfu*. Sb and As contents are negatively correlated. The presence of Fe, S, and Cl was detected only in few spot analysis, not exceeding

Table 3. Chemical composition of kermesite from Pernek.

	Kermesite, Pernek			
	mean	range	^{*2}	^{*3}
Pb	0.06	0.00–0.10	0.001	
Zn	0.02	0.00–0.09	0.001	
Sb	74.56	74.13–74.99	1.979	75.24
As	0.44	0.00–1.23	0.019	
Cl	0.01	0.00–0.02	0.001	
S	19.83	19.57–19.96	1.998	19.81
$O^{*1}_{calc.}$	4.96	4.90–5.01	1.002	4.94
Total	99.85			100.00

^{*1} Oxygen content calculated on the basis $O = 1$ at ideal formula Sb_2S_2O; ^{*2} atoms per formula unit (*apfu*) on the basis of 5 atoms; ^{*3} calculated composition on the basis ideal formula Sb_2S_2O.

0.04 wt. %. The calculated formula $(Sb_{1.99}As_{0.01})_{\Sigma 2.00}O_3$ agrees well with ideal composition of Sb_2O_3. The refined unit-cell parameters are $a = 4.913(1), b = 12.470(3), c = 5.429(3)$ Å.

Kermesite forms lath-shaped crystals, up to 1 cm long and 5–50 µm thick. These crystals are intergrown in sheaflike aggregates, up to 1.5 cm long, or radiating groups, 0.5–1.0 cm large. Splinters and thin edges of kermesite are translucent, with abundant red internal reflections. Kermesite is sectile, with perfect {001} cleavage and brownish-red streak. Thin splinters are flexible. Electron microprobe analyses (Table 3) indicated presence of Sb, and S. Impurities in the studied kermesite specimens include up to 0.053 *apfu* As and less than 0.10 wt. % of Pb, Zn and Cl. Sb and As are negatively correlated. The calculated formula $(Sb_{1.98}As_{0.02})_{\Sigma 2.00}S_{2.00}O_{1.00}$ agrees well with the ideal composition Sb_2S_2O. Small As concentration was also reported from kermesite from the nearby Sb deposit Pezinok (Cambel, 1959). The refined unit-cell parameters are $a = 8.156(6), b = 10.714(7), c = 5.791(3)$ Å, $\alpha = 102.74(4)°$, $\beta = 110.62(4)°$, $\gamma = 100.99(5)°$.

Senarmontite was formed at least during two separate stages. The earlier senarmontite (I) forms octahedral crystals, usually 0.2–1.0, rarely up to 2–3 mm large. The crystals are colorless, grayish white or gray, translucent to transparent, with resinous luster. They postdate crystals and masses of ankerite, occasionally are intergrown with berthierite, and precede the crystallization of kermesite and schafarzikite. Later senarmontite (II) is found on fractures of ores as white crusts composed of subhedral crystals (< 0.1 mm large) with pearly luster. No cleavage planes were observed. BSE images of senarmontite (I) show a chemically homogeneous phase with abundant inclusions of acicular crystals of berthierite. A single senarmontite crystal may contain tens of berthierite inclusions. Chemical impurities include only minor Ca and Fe (Table 2). The refined unit-cell parameter is $a = 11.1504(4)$ Å.

Gypsum was found only on a single hand specimen. Transparent tabular crystals, up to 10 mm long, cover an area of 1 × 1 cm^2. Gypsum is clearly one of the youngest minerals. It encloses minute acicular crystals of kermesite. Identification was verified by an XRD analysis.

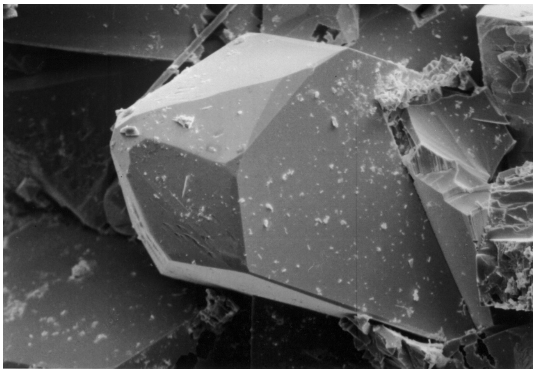

Fig. 3. Scanning electron photomicrograph of a short columnar schafarzikite crystal from Pernek. (Tesla BS 320, J. Sejkora & A. Gabašová; field of view 400 µm).

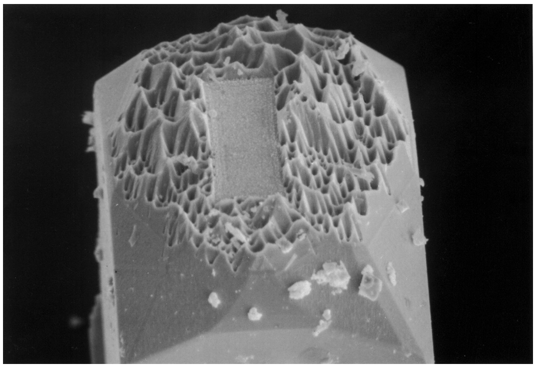

Fig. 4. Scanning electron photomicrograph of terminal portion of the schafarzikite crystals with negative imprints of tabular valentinite and acicular kermesite. (Tesla BS 320, J. Sejkora & A. Gabašová; field of view 120 µm).

Crystal morphology of schafarzikite and its relationship to other minerals

Schafarzikite forms isolated crystals and druses of randomly oriented individuals, covering areas up to 1×2 cm^2. Relatively common mode of occurrence are also crystalline crusts, up to 2 mm thick and 2×3 cm^2 in area. Schafarzikite crystals are prismatic (Fig. 3), usually only 0.1–1.0 mm long, rarely as long as 1.5 mm. The dominant form is {110}, other forms are {121}, {112}, {010}, {221}, {131}, {231}, and several unindexed forms. Striation parallel to [001] (Anthony *et al.*, 1997) was not observed. Terminal portions of schafarzikite crystals often display negative imprints of acicular crystals of kermesite and less commonly also probably valentinite (Fig. 4).

Schafarzikite occurs on fractures of the ores in association with numerous Fe-Sb sulfides and oxides. The earliest minerals are ankerite and stibnite. Crystallization of stibnite preceded the formation of parallel overgrowths of valentinite (I) and precipitation of senarmontite (I) and berthierite. In a following stage, schafarzikite and kermesite crystallized simultaneously. The formation interval of valentinite (II) probably slightly overlaps with that of kermesite and schafarzikite. However, most valentinite (II) formed after kermesite and schafarzikite. Crystalline crusts

Table 4. Chemical composition of schafarzikite.

	FeO	ZnO	PbO	As_2O_3	Sb_2O_3	Bi_2O_3	SO_2	Cl	Total
mean	19.38	0.02	0.02	0.55	80.36	0.16	0.04	0.00	100.53
*1	19.25	0.06	0.00	0.33	80.76	0.00	0.04	0.01	100.44
*1	19.25	0.00	0.08	0.00	80.29	0.00	0.06	0.00	99.68
*1	19.30	0.00	0.00	0.50	80.25	0.33	0.02	0.00	100.39
*1	19.31	0.00	0.05	1.01	79.89	0.00	0.06	0.00	100.33
*1	19.33	0.00	0.00	0.26	80.70	0.38	0.04	0.00	100.72
*1	19.34	0.12	0.05	0.32	80.61	0.32	0.03	0.00	100.79
*1	19.35	0.04	0.00	0.28	80.74	0.00	0.04	0.00	100.45
*1	19.37	0.05	0.00	0.84	80.91	0.29	0.04	0.00	101.50
*1	19.37	0.00	0.00	0.34	79.04	0.23	0.05	0.02	99.06
*1	19.42	0.00	0.00	1.42	80.06	0.49	0.08	0.01	101.48
*1	19.47	0.00	0.06	0.83	80.25	0.00	0.04	0.00	100.65
*1	19.50	0.00	0.06	0.61	80.88	0.00	0.04	0.01	101.09
*1	19.67	0.00	0.00	0.36	80.24	0.00	0.04	0.00	100.31
*2	19.77				80.23				100.00
*3	38.20				61.30				99.50
*4	17.58	1.10		9.72	67.95				96.35
*5	0.974	0.001	0.000	0.022	1.991	0.002	0.003	0.000	

*1: 13 point analyses of schafarzikite from Pernek (this paper); *2: theoretical composition; *3: schafarzikite, Pernek (Hueber, 1932); *4: schafarzikite, Buca della Vena (Mellini *et al.,* 1979); *5: atoms per formula unit (*apfu*) on the basis of 4 oxygens.

of senarmontite (II) represent the final stages of precipitation of Fe-Sb minerals. The youngest mineral among those accompanying schafarzikite is gypsum.

Physical properties of schafarzikite

Schafarzikite from Pernek is dark brown to almost black, translucent only in very thin fragments. In reflected light, red internal reflections are much less abundant than in associated kermesite. Schafarzikite is uniaxial, with parallel extinction, negative optic sign, and pleochroism in reddish-brown tints. The refraction indices are higher than 1.74, in agreement with measurements of Tokody (1925) and Zemann (1951). The average refraction index, calculated from the Gladstone-Dale equation, is N = 2.001. Schafarzikite from Pernek has adamantine to metallic luster, brown streak, and is brittle. Several planes of excellent cleavage are parallel with the z axis; in addition, good {100} cleavage can be observed. Microhardness was measured on two grains with different crystallographic orientation. The first grain was a cut in zones [110] and [010] with numerous traces of parallel cleavage planes. The average of 11 experiments gave $VHN_{5g} = 251$ kp/mm^2 (2461 N/mm^2). The second grain was a cut perpendicular to (001), with fewer traces of intersecting cleavage planes and triangular pits. Sixteen measurements averaged $VHN_{10g} = 278$ (229–343) kp/mm^2, *i.e.*, 2726 (2246–3364) N/mm^2, $K_{VH} = 1.50$. These microhardness values correspond to hardness of 3.5–4.0 on the Mohs' scale, in good agreement with the hardness of 3.5 determined by Tokody (1925). Schafarzikite is neither fluorescent under long- and short-wave ultraviolet radiation, nor cathodoluminiscent. Density was not measured because of paucity of the material. Calculated density of 5.507 g/cm^3 is significantly greater than the experimental value of 4.3 g/cm^3, stated by Tokody (1925).

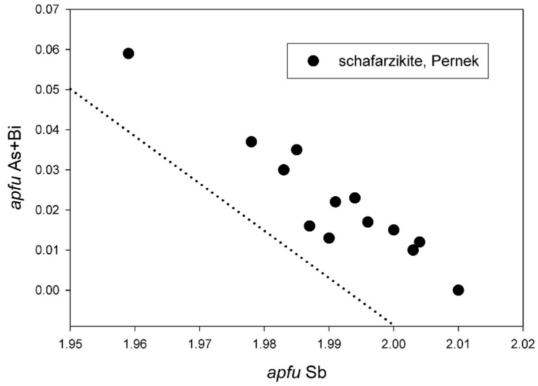

Fig. 5. The relation of Sb and As+Bi contents in schafarzikite from Pernek; the dotted line represent the ideal ratio Sb:(As+Bi) = 1:2.

Chemical composition

The formula for schafarzikite from Pernek is $Fe_{0.97}(Sb_{1.99}As_{0.02})_{\Sigma 2.01}O_4$ (mean of 13 point analyses – Table 4), close to the ideal composition $FeSb_2O_4$. No zonality or inclusions were visible in BSE images.

Arsenic concentration in schafarzikite from Pernek does not exceed 0.059 *apfu*, but Mellini *et al.* (1979) found up to 0.356 *apfu* As in schafarzikite from Buca della Vena. The concentrations of Sb and (As+Bi) are negatively correlated (Fig. 5); the deviation from the ideal negative correlation are owing to the deficiency on the Fe site. Minor As content was also determined in the coexisting valentinite and kermesite (see above). Traces of As have been reported also from kermesite and stibnite from a nearby deposit Pezinok (Cambel, 1959). Andráš *et al.* (1993) found rare minerals of bismuth in Pezinok.

A characteristic feature of schafarzikite from Pernek is the deficiency on the Fe site, which is occupied only

Table 5. X-ray powder diffraction pattern of schafarzikite.

			Pernek^{*1}			Buca della Vena^{*2}	
h	*k*	*l*	d_{obs}	I/I_o	d_{calc}	d_{obs}	I/I_o
1	1	0	6.083	12	6.086	6.04	21
2	0	0	4.302	38	4.304	4.28	59
2	1	0	3.847	4	3.849		
2	1	1	3.224	100	3.225	3.209	100
2	2	0	3.042	65	3.043	3.031	50
0	0	2	2.954	6	2.955	2.937	10
3	1	0	2.721	76	2.722	2.708	50
1	1	2	2.659	10	2.658	2.643	5
2	0	2	2.436	15	2.436	2.423	9
2	1	2	2.344	4	2.344	2.330	3
4	0	0	2.152	6	2.152	2.138	3
4	1	0	2.087	3	2.088		
3	3	0	2.029	43	2.029	2.021	13
3	1	2	2.002	5	2.002		
4	1	1	1.9682	87	1.9684	1.960	29
4	2	0	1.9246	21	1.9247	1.915	12
2	1	3	1.7535	10	1.7535	1.744	5
4	0	2	1.7393	9	1.7394	1.731	4
3	3	2	1.6724	29	1.6725	1.665	11
5	2	1	1.5428	23	1.5429	1.537	4
4	4	0	1.5215	8	1.5216	1.516	3
0	0	4	1.4769	3	1.4773		
5	3	0	1.4760	25	1.4761	1.470	16
5	1	2	1.4656	10	1.4657		
6	0	0	1.4347	29	1.4346	1.428	15
4	1	3	1.4329	21	1.4327		
6	1	0	1.4148	3	1.4150		
2	0	4	1.3972	2	1.3973		
6	2	0	1.3608	5	1.3609		
5	4	0	1.3440	3	1.3442		
2	2	4	1.3287	2	1.3290		
5	3	2	1.3204	7	1.3205		
5	4	1	1.3106	24	1.3108		
3	1	4	1.2986	4	1.2984		
6	0	2	1.2907	6	1.2905		
5	2	3	1.2412	5	1.2411		
6	2	2	1.2361	9	1.2361		
3	3	4	1.1940	2	1.1943		
4	2	4	1.1722	2	1.1719		
7	2	1	1.1593	13	1.1593		
7	3	0	1.1304	3	1.1302		
2	1	5	1.1295	3	1.1298		
5	5	2	1.1257	7	1.1255		
5	4	3	1.1103	7	1.1103		
6	4	2	1.1069	11	1.1067		
8	0	0	1.0759	2	1.0759		
8	1	1	1.0506	17	1.0506		
7	4	1			1.0506		
5	3	4	1.0445	6	1.0445		
8	2	0	1.0437	4	1.0438		
6	0	4	1.0292	6	1.0292		
4	1	5	1.0287	4	1.0285		
6	6	0	1.0143	4	1.0144		
7	2	3	1.0137	7	1.0137		
8	0	2	1.0111	11	1.0111		

^{*1} This study; ^{*2} Buca della Vena, Italy (Mellini *et al.,* 1979).

at 0.974 *apfu*. Similarly, this position is occupied by 0.935 *apfu* (Fe+Zn) in schafarzikite from Buca della Vena (Mellini *et al.,* 1979). The presence of structural domains resembling versiliaite or apuanite (Mellini *et al.*, 1981) in our samples is unlikely, because the Fe occupancy is only 0.974 *apfu*, and S concentration is not greater than 0.004 *apfu*.

The first published analysis of schafarzikite from Pernek (Hueber, 1932) is very likely incorrect. Hueber's data are tens of per cent off from any other published analyses, and the Fe:Sb ratio is about 5:4, indicative of a phase close to tripuhyite (Fe:Sb = 1:1) rather than schafarzikite (Fe:Sb = 1:2).

X-ray powder diffraction study

Positions of the XRD peaks for our schafarzikite sample (Table 5) agree with the published data and the pattern calculated from crystal structure refinement (Fischer & Pertlik, 1975). However, the experimental intensities of (*hh*0), (*hk*0), and (*h*00) peaks are about 5–8 times higher than those in the calculated pattern, most likely due to preferred orientation. The measured intensities are in much better agreement with the experimental data of Mellini *et al.* (1979), suggesting that the preferred orientation is caused by orientation of the cleavage fragments of schafarzikite.

Table 6. Unit-cell parameters of schafarzikite (space group $P4_2/mbc$).

	Pernek	Pernek	Pernek	Bucca della Vena	synthetic $FeSb_2O_4$
	this paper	Zemann (1951)	Fischer & Pertlik (1975)	Mellini *et al.* (1979)	Chater & Gararri (1985)
a	8.6073(2)	8.59(2)	8.590(5)	8.568(4)	8.612
c	5.9093(3)	5.92(2)	5.913(5)	5.96(1)	5.917
V	437.80(2)	436.8	436.3	437.3	438.9
c : *a*	0.6865	0.6892	0.6884	0.6956	0.6871

The refined unit-cell parameters for schafarzikite from Pernek (Table 6) agree with the data for synthetic $FeSb_2O_4$ (Chater & Gararri, 1985). The slight differences between the unit-cell parameters of schafarzikite from Pernek (this study, Fischer & Pertlik, 1975) and schafarzikite from Buca della Vena (Mellini *et al.,* 1979) are likely owing to isomorphous substitution of As or Mn in the structure. The *c* : *a* ratio of 0.6865 corresponds well to the values of 0.692 (Krenner, 1921) and 0.674 (Tokody, 1925, Zemann, 1951), both determined from observation of crystal morphology.

Table 7. Thermal analyses of schafarzikite from Pernek.

Temperature	Mass increase			*1	*2
20 °C–580 °C	0.048 mg	1.62 wt. %	+2.16 wt. %	$Fe^{2+} \rightarrow Fe^{3+}$	+2.16 wt. %
			−0.54 wt. %	As_2O_3 release	−0.55 wt. %
580 °C–850 °C	0.157 mg	5.28 wt. %	+5.28 wt. %	$Sb^{3+} \rightarrow Sb^{5+}$	+5.29 wt. %

Sample weight 2.968 mg, heating rate 10 °C.min^{-1} in flowing air. *1 Tentative interpretation of thermal behaviour of schafarzikite; *2 Theoretical values calculated from the proposed scheme of thermal decomposition of schafarzikite (60 % of Sb^{3+} oxidized to Sb^{5+}).

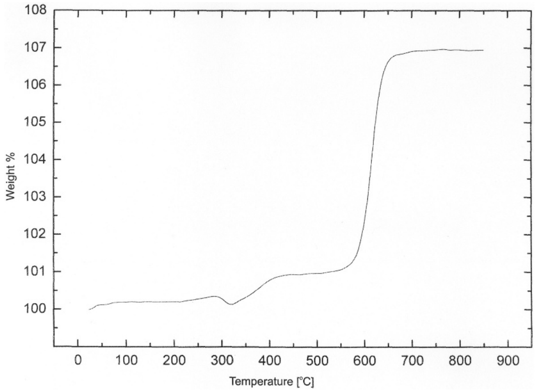

Fig. 6. Thermogravimetric curve of schafarzikite from Pernek.

Thermogravimetric analysis

The weight gains and losses of schafarzikite during heating (Fig. 6) are tabulated in Table 7. The sample weight increases because of oxidation of Fe^{2+} and Sb^{3+} and associated incorporation of oxygen from air in the sample. Divalent iron is fully oxidized to Fe^{3+} ($Fe^{2+} \Rightarrow Fe^{3+}$). The thermogravimetric trace shows that only ~ 60 % of Sb^{3+} (1.2 Sb *apfu* of schafarzikite) is oxidized to Sb^{5+} ($Sb^{3+} \Rightarrow Sb^{5+}$). Thus, the phase formed by heating is a member of solid solution series in the system Fe^{3+}-Sb^{3+}-Sb^{5+}-O. This interpretation is consistent with a coupled substitution $M^{3+} + M^{5+} \Leftrightarrow 2\ M^{4+}$, known also from synthetic pigments with rutile ($Ti^{4+}O_2$) structure (Makarov, 1973, Wells, 1986). A small weight loss is most likely due to liberation of volatile As compounds from the sample. The XRD pattern of brown product of the thermal decomposition of schafarzikite is structurally related to tripuhyite ($Fe^{3+}Sb^{5+}O_4$), a mineral isostructural with rutile (Basso *et al.*, 2003; Berlepsch *et al.*, 2003). Thus, mechanism of the thermal decomposition of schafarzikite may be described by a schematic equation

$$Fe^{2+}(Sb_{1-x}As_x)_2^{3+}O_4\ (s) + O_2\ (g) \Rightarrow$$
$$Fe^{3+}Sb^{3+}_{0.8}Sb^{5+}_{1.2}O_{5.7}(s) + 0.5x\ As_2O_3(g)$$

Infrared and Raman spectra

The FTIR and Raman spectra of schafarzikite from Pernek are shown in Figs. 7 and 8, respectively. Band positions, intensities, and tentative assignments are listed in Table 8.

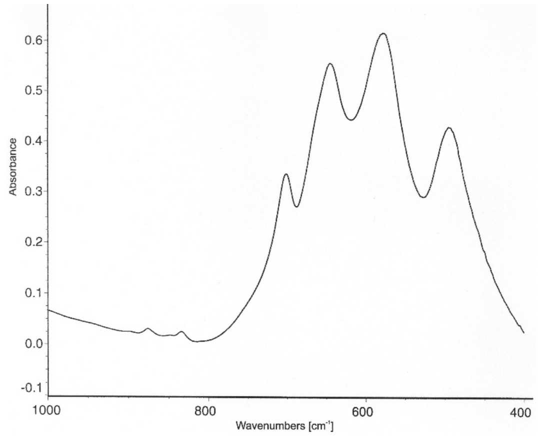

Fig. 7. Infared spectrum of schafarzikite from Pernek.

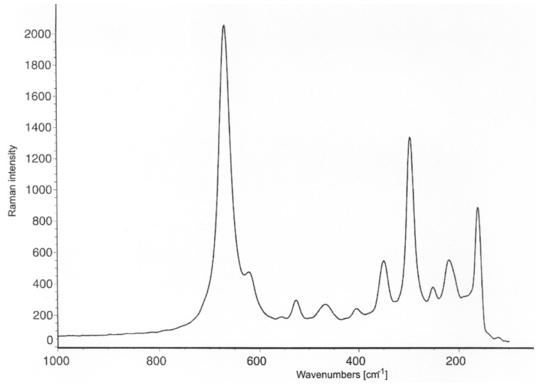

Fig. 8. Raman spectrum of schafarzikite from Pernek.

To our knowledge, vibrational spectra for schafarzikite or synthetic $FeSb_2O_4$ have not been published.

Assignment of the vibrational bands is based on the results of Plyusnina (1976), Nandini Devi & Vidyasagar (1998), Ruan *et al.* (2001), and theoretical calculations and experimental data of Gilliam *et al.* (2004). Bands near 700 cm^{-1} and 252 cm^{-1} were assigned to the Sb-O-Sb stretching vibrations. Bands in the region 610–670 cm^{-1} and 405–467 cm^{-1} were attributed to the Fe-O-Fe stretching vibrations. Bands near 580 cm^{-1} may be connected with the Fe-O-Fe stretching vibrations or Fe-O terminal vibrations. Band in at 497 cm^{-1} may be attributed to the Sb-O-Fe stretching vibrations, and/or the Fe-O-Fe stretching and/or Sb-O terminal vibrations. Bands observed in the range 295–405 cm^{-1} and 161–217 cm^{-1} may be assigned to the Sb-O-Sb bending vibrations and those at 252 cm^{-1} to the Fe-O-Fe bending vibrations.

Table 8. Infrared and Raman spectra of schafarzikite.

Infrared [cm^{-1}]		Raman [cm^{-1}]		Tentative assignment
703	s			Sb-O-Sb stretch
		670	vs	
646	vs			Fe-O-Fe stretch
		617	wm	
579	vs			Fe-O-Fe stretch or Fe-O terminal
		524	w	
497	svs			Sb-O-Fe strech or Sb-O terminal or FeO-Fe stretch
		467	w	Fe-O-Fe stretch or Sb-O-Sb stretch
		405	w	
		348	m	Sb-O-Sb bend
		295	s	
		252	wm	Fe-O-Fe bend or Sb-O-Sb stretch
		217	m	
		161	ms	Sb-O-Sb bend

Intensity of IR and Raman bands: vs - very strong; s - strong; m - medium; w - weak; vw - very weak.

Notes about formation of schafarzikite

The association of valentinite (I), senarmontite (I), kermesite, and schafarzikite was probably formed from late oxidizing hydrothermal fluids. A similar genesis was hypothesized for kermesite and valentinite from a nearby Sb deposit Pezinok (Cambel, 1959). The younger assemblage of valentinite (II) and senarmontite (II) is very likely also hydrothermal. The only supergene phase among the observed minerals is gypsum.

The hypothesis about primary, hydrothermal origin of the Fe-Sb-S-O minerals is supported by:

- probably parallel intergrowths of valentinite (I) and stibnite;
- absence of pseudomorphs of kermesite or valentinite after stibnite;
- absence of fully oxidized phases stable in contact with atmospheric oxygen levels, such as Fe^{3+} oxyhydroxides (*e.g.*, goethite) or Sb^{5+} ochres (*e.g.*, cervantite, stibiconite). Only minerals with Fe^{2+} (schafarzikite) and Sb^{3+} (kermesite, schafarzikite, senarmontite, valentinite) are present;
- absence of hydrated or hydroxylated phases among the Fe-Sb minerals.

Acknowledgements: The paper has been financially supported as part of the research grant projects 205/03/D004, MK00002327201 and VEGA 1/2028/05. We are thankful to J. Litochleb (National Museum, Prague), M. Novotná, J. Poledna a J. Ederová (Vysoká škola chemicko-technologická, Prague), the late A. Gabašová (Czech Geological Survey, Prague) and M. Huraiová (Comenius University, Bratislava) for extensive help with the instrumental methods used in this work. We thank J. Majzlan (Princeton University) for editorial comments on the English version of the manuscript.

References

Andráš, P., Jeleň, S., Caňo, F. (1993): Occurrence of Bi-mineralization at the deposit Pezinok. *Min. Slovaca*, **25**, 221-223 (in Slovak).

Anthony, J.W., Bideaux, R.A., Bladh, K.W., Nichols, M.C. (1997): Handbook of Mineralogy. Vol. III. Halides, hydroxides, oxides. 628 p., Mineral. Data Publ., Tucson.

Basso, R., Cabella, R., Lucchetti, G., Marescotti, P., Martinelli, A. (2003): Structural studies on synthetic and natural Fe-Sb-oxides of MO$_2$ type. *N. Jb. Miner. Mh.*, **9**, 407-420.

Berlepsch, P., Armbruster, T., Brugger, J., Criddle, A.J., Graeser, S. (2003): Tripuhyite, FeSbO$_4$, revisited. *Mineral. Mag.*, **67**, 1, 31-46.

Blackburn, W.H. & Dennen, W.H. (1997): Encyclopedia of Mineral Names. Special Publication 1 of The Canadian Mineralogist. Miner. Assoc. Canada, Ottawa, 1-360.

Burnham, Ch.W. (1962): Lattice constant refinement. *Carnegie Inst. Washington Year Book*, **61**, 132-135.

Callegari, A. & Mattioli, V. (2000): Schafarzikite from Alpe Stabiello (Sondrio Province). *Rivista Mineralogica Italiana*, **4**, 255-256.

Cambel, B. (1959): Hydrothermal deposit in the Malé Karpaty Mts. Mineralogy and geochemistry of their ores. *Acta Geol. Geograph. Univ. Comen., Geol.*, **3**, SPN, Bratislava, 1-348 (in Slovak).

Cambel, B., Král', J., Bruchart, J. (1990): Isotope geochrology of the Western Carpathians crystalline complex. VEDA, Bratislava, 1-183 (in Slovak).

Chater, R., Gavarri, J.R., Hewat, A. (1985): Structures isomorphes MeX$_2$O$_4$ - Evolution structurale entre 2 K et 300 K de l'antimonite $FeSb_2O_4$: Elasticité et ordre magnétique anisotropes. *J. Solid State Chem.*, **60**, 78-86.

Čillík, I., Sobolič, P., Žákovský, R. (1959): Notes about the tectonic structure of the Pezinok-Pernek crystalline komplex. *Geol. Práce, Zprávy*, **15**, 43-64.

Dill, H.G., Weiser, T., Bernhardt, I.R., Kilibarda, C.R. (1995): The composite gold-antimony vein deposit at Kharma (Bolivia). *Econ. Geol.*, **90**, 51-66.

Fischer, R. & Pertlik, F. (1975): Verfeinerung der Kristallstruktur des Schafarzikits, $FeSb_2O_4$. *Tschermaks Mineral. Petrog. Mitt.*, **22**, 236-241.

Gilliam, S.J., Jensen, J.O., Banerjee, A., Zeroka, D., Kirkby, S.J., Merrow, C.N. (2004): A theoretical and experimental study of Sb_4O_6: vibrational analysis, infrared, and Raman spectra. *Spectrochim. Acta*, **A60**, 425-434.

Hueber, H. (1932): Über die Anwendung von Mikromethoden in der Mineralanalyse. *Zbl. Miner. Geol. Paläont., Abt. A. (Stuttgart)*, 337-344.

Koděra, M. *et al.* (eds.) (1990): Topographical mineralogy of Slovak Republic II. VEDA, Bratislava, 585-1098 (in Slovak).

Krenner, J.A. (1921): Schafarzikit, ein neues Mineral. *Z. Kristallogr.*, **56**, 198-200.

Krenner, J.A. (1923): Schafarzikit, egy új magyar ásvány. *Math. természet. Tudom. Ért (Budapest)*, **41**, 255-258.

Makarov, E.S. (1973): Isomorphism of atoms in crystals. Atomizdat Moscow (in Russian).

Mellini, M., Amouric, M., Baronnet, A., Mercuriot, G. (1981): Microstructures and nonstoichiometry in schafarzikite-like minerals. *Am. Mineral.*, **66**, 1073-1079.

Mellini, M., Merlino, S., Orlandi, P. (1979): Versiliaite and apuanite: two new minerals from the Apuan Alps, Italy. *Am. Mineral.*, 64, 1230-1234.

Nandini Devi, R. & Vidyasagar, K. (1998): Synthesis and characterization of new vanadates of antimony $ASbV_2O_8$ (A = K, Rb, Tl of Cs). *J. Chem. Soc. Dalton Trans.*, **18**, 3013-3019.

Planderová, E. & Pahr, A. (1983): Biostratigraphical evaluation of weakly metamorphosed sediments of Wechsel series and their possible correlation with Harmónia Group in Malé Karpaty Mts. *Min. Slovaca*, **15**, 5.

Plašienka, D., Michalík, J., Kováč, M., Gross, P., Putiš, M. (1991): Paleotectonic evolution of the Malé Karpaty Mts - an overview. *Geol. Carpath.*, **42**, 4, 195-208.

Plyusnina, I.I. (1976): Infrared spectra of minerals. Moscow University Publishers, 175 p. (in Russian).

Robinson, G.W. & Normand, Ch. (1996): The Lac Nicolet antimony mine, South Ham, Québec. *Mineral. Record*, **27**, 121-134.

Ruan, H.D., Frost, R.L., Kloprogge, J.T. (2001): The behaviour of hydroxyl units of synthetic goethite and its dehydroxylated product hematite. *Spectrochim. Acta*, **A57**, 2575-2586.

Tokody, L. (1925): VI. Beitrage zur Kenntnis der kristallographischen und physikalischen Eigenschaften des Schafarzikits. *Z. Kristallogr.*, **62**, 123-126.

Wells, A.F. (1986): Structural inorganic chemistry, 5*th* Ed., Clarendon Press, Oxford.

Yvon, K., Jeitschko, W., Parthé, E. (1977): Lazy Pulverix, a computer program for calculation X-ray and neutron diffraction powder patterns. *J. Appl. Cryst.*, **10**, 73-74.

Zemann, J. (1951): Formel und Kristallstruktur des Schafarzikits. *Tschermaks Mineral. Petrog. Mitt.*, **2**, 166-175.

Received 29 December 2006
Modified version received 24 January 2007
Accepted 9 March 2007